INTERNATIONAL JOURNAL OF HYDROGEN ENERGY XXX (2017) 1–8

Available online at www.sciencedirect.com

ScienceDirect

journal homepage: www.elsevier.com/locate/he

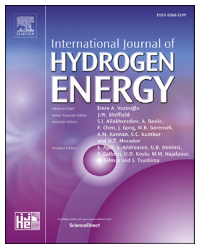

Short Communication

MHD mixed convection flow along a vertically heated sheet

Rizwan Ul Haq [a,*], *Zakia Hamouch* [b], *S.T. Hussain* [c], *Toufik Mekkaoui* [b]

[a] *Department of Electrical Engineering, Bahria University, Islamabad, Pakistan*
[b] *Department of Mathematics, Faculty of Science and Technology, Errachidia, Morocco*
[c] *DBS&H, CEME, National University of Sciences and Technology, Islamabad, Pakistan*

ARTICLE INFO

Article history:
Received 12 January 2017
Received in revised form
13 April 2017
Accepted 21 April 2017
Available online xxx

Keywords:
Mixed convection
MHD
Porous medium
OHAM
Numerical solution

ABSTRACT

Main objective of this frame work is to establish the modeling and simulation of mix convection flow along a vertically heated sheet filled with water. Two important mechanisms: magneto-hydrodynamics and porous medium are also considered within the restricted domain of the fluid flow. Temperature is controlled with the wall temperature and then mathematical model is constructed in the form of PDEs. To determine the similarity solution results are obtained via two different techniques. Numerically solutions are obtained with the help of shooting technique and then validate with the help of optimal homotopy analysis method (OHAM). Obtained analytical and numerical results are validated graphically. Effect of emerging parameters are plotted for velocity and temperature profiles. It is found that for mixed convection parameter $(\xi < 0)$, velocity profile depicts the increasing behavior for various values of power index m. However, for $\xi > 0$, velocity profile shows the decreasing behavior with respect the parameter m. Temperature distribution in the restricted domain depicts the decreasing behavior for both m and ξ.

Introduction

Mixed convection phenomenon is of significant importance because flow is driven under the influence of dual forces. Natural convection under the effect of buoyancy force and forced convection due to the application of stress. Mixed convection is desired when only the forced convection or the natural convection is not sufficient to achieve the results. The relative contribution of natural or forced convection depends upon the flow behavior (laminar flow or turbulent flow) and temperature of the fluid. Mixed convection phenomenon has applications in several industrial and engineering processes like cooling systems, water transportation system, chemical separation instruments and electronic devices cooling process. Sparrow et al. [1], developed the similarity solutions for the mixed convective boundary layer flow. Merkin and Pop [2] considered the mixed convection flow along the vertical

* *Corresponding author.*
E-mail addresses: ideal_riz@hotmail.com, r.haq.qau@gmail.com (R. Ul Haq).
http://dx.doi.org/10.1016/j.ijhydene.2017.04.225

Please cite this article in press as: Ul Haq R, et al., MHD mixed convection flow along a vertically heated sheet, International Journal of Hydrogen Energy (2017), http://dx.doi.org/10.1016/j.ijhydene.2017.04.225

surface and obtained the similarity solution when the free stream velocity is uniform. Recently Nadeem and Saleem [3] discussed the mixed convection flow of Eyring–Powell fluid along a rotating cone. Noor et al. [4] considered the mixed convective flow of micro-polar nanofluid and discussed the effects of micro-rotation and Brownian motion on the convective heat transfer. Some recent studies also shed the light on important aspects of convective heat transfer [5,6]. Another important aspect can be the study of mixed convection in porous media. Heat transfer process in porous media is involved in several processes like transpiration cooling, separating chemicals in industrial process, filtration process in aquifers, storage and transport of nuclear waste material etc. Nield and Bejan [7], Ingham and Pop [8] and Vafai [9] books explored different aspects of convection in porous media and its industrial applications. Kumaran and Pop [10] referred to an important aspect that most of the studies considered the mixed convection at the normal temperature where the density of the fluid is constant and the Boussinesq approximation is valid. Fluid density does vary with the change in temperature. Water has the maximum density of 999.97 kg m^{-3} at 4 °C [11]. For temperature greater than 4 °C, the density of water decreases with the increase in temperature. However, for temperature less than 4 °C the density of water increase with the increase in temperature and has the maximum density at 4 °C. The maximum density of water ρ_c in liquid state is attained at the temperature $T_c = 3.98$ °C. Goren [12] has shown that the relationship between the density and the temperature is given by $\frac{\rho-\rho_c}{\rho_c} = -\gamma(T-T_c)^2$, where $\gamma = 8 \times 10^{-6}(°C)^{-2}$ is the fluid thermal expansion coefficient of water at 4 °C. Moore and Weiss [13] stated that above equation is accurate within the range $0°C \leq T \leq 8$ °C with the precision ±4%. For wider range of temperatures, Gebhart and Mollendorf [14] propose another relation but in present article, the above-mentioned relation is used. For small temperature variations around T_c the free convection, motion is relatively small and it can be an important consideration in cooling systems where the interest lies in reducing the free convection like coolants and energy plants.

In cooling systems, another important aspect is the effect of magnetic field along with the mixed convection flow. Georgantopoulos et al. [15] considered the oscillatory convective flow of water at 4 °C along an infinite porous plate. Takhar and Perdikis [16] studied the magnetic field effects on the free convective flow of water past an infinite porous plate. Recently Xenos et al. [17] discussed the free convective MHD flow of water at 4 °C along a vertically permeable surface. Finite volume discretization method is used to solve developed mathematical problem. It is reported that in free convective flow the velocity decrease due to the presence of magnetic field. Present article is aimed to explore the mixed convective flow of water at its maximum density (i.e at 4 °C) in the porous media for the three cases namely; Variable wall temperature, Variable Heat flux and Variable heat transfer coefficient. These three conditions are assumed in such a way that the temperature of the wall, heat flux and the heat transfer coefficient are changing proportionally to space variable along the plate. Moreover, variable free stream velocity is considered which is changing along the coordinates of the plate. Recent studies indicate the magnetohydrodynamics effects for various physical models [18–24]. Apart from mentioned studies, recently essential part of research is focusing to convert the chemical energy into electricity from fuel cells and these studies presented by various authors [25–29].

This study governs the mix convection flow of water at 4 °C along a vertically plat. Two important mechanisms: magnetohydrodynamics and porous medium are also considered with the surface of the plat. The major format of the whole study is defined in the following sections. In section two, mathematical model is constructed according to the defined geometry. In section three, a convergence criterion is obtained via OHAM. Numerical method for present study is defined in section four and result and discussion are analyzed in the last section.

Mathematical model

Consider the steady incompressible flow of mixed convection fluid along a vertically semi-infinite surface. It is further considered that semi-infinite region fenced with the porous medium that is filled with the working fluid water at 4 °C. A uniform magnetic field is applied normal to the surface of the vertical plate and temperature of the surface is controlled with three various way namely: variable wall temperature (VWT), variable heat transfer coefficient (VHF), and variable heat transfer coefficient (VHTC). The ambient fluid temperature is considered to be $T_\infty = T_c$; while rest of fluid embedded in porous media is constant. For simplicity Cartesian coordinate system (x, y) is adjusted in such a way that x-axis is considered vertically and y-axis is taken horizontally. The

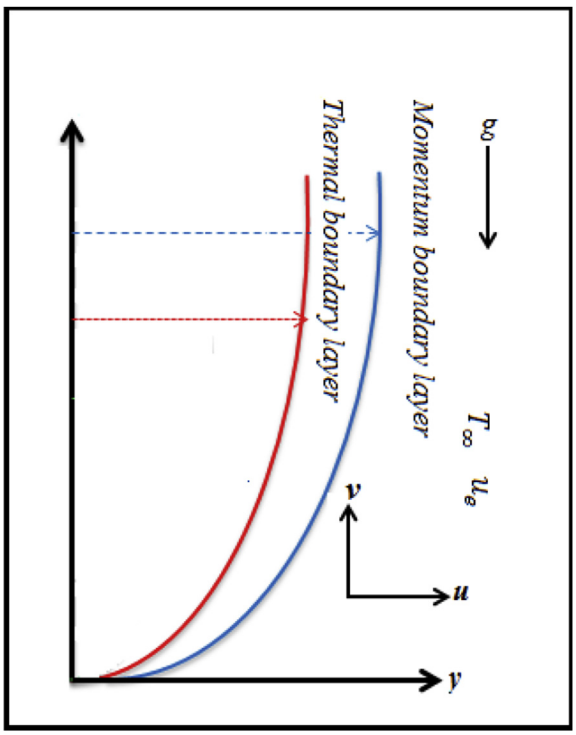

Fig. 1 – Geometry of the model.

Please cite this article in press as: Ul Haq R, et al., MHD mixed convection flow along a vertically heated sheet, International Journal of Hydrogen Energy (2017), http://dx.doi.org/10.1016/j.ijhydene.2017.04.225

plate $y = 0$ is located parallel to the free stream velocity $u_e = u_\infty x^{2m}$; oriented in the upward direction such that m is a scalar quantity (shown in Fig. 1). The governing boundary layer equations in the presence of Boussinesq approximation are [5,30]:

$$\frac{\partial u}{\partial x} + \frac{\partial u}{\partial y} = 0, \tag{1}$$

$$\overbrace{(u-u_e)\frac{\mu}{k\rho_c}}^{\text{For Porous media}} + \overbrace{(u-u_e)\frac{\sigma B_0^2}{\rho_c}}^{\text{For MHD}} = \overbrace{\pm g\gamma(T-T_c)^2}^{\text{For mixed convection}}, \tag{2a}$$

Simplified form of Eq. (2a) is represented as:

$$u = u_e \pm \frac{gk\gamma\rho_c}{\mu + \sigma k B_0^2}(T-T_c)^2, \tag{2b}$$

$$u\frac{\partial T}{\partial x} + v\frac{\partial T}{\partial y} = \alpha_m \frac{\partial^2 T}{\partial y^2}, \tag{3}$$

where u and v are the velocity components and T is the temperature of fluid. The compatible boundary conditions are defined as:

$$v(x,0) = 0, u(x,y) \to u_e(x) \text{ or } (T(x,y) \to T_c) \text{ as } y \to \infty. \tag{4}$$

The constants μ, k, α_m, g, σ, γ and B_0 are, viscosity, permeability, thermal diffusivity, gravitational acceleration, the electric conductivity, thermal expansion coefficient and applied magnetic field, respectively. The plus sign inEq. (2b) accounts the assisting flows and the minus sign represent the opposing flows. Since, three various wall conditions: (i) variable wall temperature, (ii) variable heat flux and (iii) variable heat transfer coefficient are considered so, Eqs. (1)–(4) will be solved under one of the following conditions [10]:

$$\text{(i)} \quad (VWT)\ \frac{T(x,0)-T_c}{T_c} = x^m, \tag{5a}$$

$$\text{(ii)} \quad (VHF)\frac{-1}{T_c}\frac{\partial T}{\partial y}(x,0) = x^{(4m-1)/2}, \tag{5b}$$

$$\text{(iii)} \quad (VHF)\ \frac{-1}{T-T_c}\frac{\partial T}{\partial y}(x,0) = x^{(2m-1)/2}. \tag{5c}$$

Stream function ψ, in the usual way as $(u,v) = \left(\frac{\partial \psi}{\partial y}, -\frac{\partial \psi}{\partial x}\right)$ that automatically satisfy Eq. (1), while Eqs. (2b) and (3) takes the following form

$$\frac{\partial \psi}{\partial y} = u_e \pm \frac{gk\gamma\rho_c}{\mu + \sigma k B_0^2}(T-T_c)^2, \tag{6}$$

$$\frac{\partial \psi}{\partial y}\frac{\partial T}{\partial x} - \frac{\partial \psi}{\partial x}\frac{\partial T}{\partial y} = \alpha_m \frac{\partial^2 T}{\partial y^2}, \tag{7}$$

Introducing the following similarity transformations [5,10].

$$\psi(x,y) = \alpha_m Pe_x^{1/2} f(\eta),\ T(x,y) = T_c[1 + x^m\theta(\eta)],\ \eta = \frac{y}{x}Pe_x^{1/2}. \tag{8}$$

where $Pe_x = \frac{u_e(x)x}{\alpha_m}$ is the local Peclet number. Hence, we obtain

$$f'(\eta) = 1 + \xi\theta(\eta)^2, \tag{9a}$$

$$\theta''(\eta) + \frac{1+2m}{2}f(\eta)\theta'(\eta) - mf'(\eta)\theta(\eta) = 0, \tag{9b}$$

and

$$f(0) = 0, f'(\eta) \to 1 (\text{or } \theta(\eta) \to 0) \text{ as } \eta \to \infty. \tag{10}$$

where, $\xi = \xi(x)$ is the mixed convection parameter that contain, Hartmann number, modified Rayleigh number and Peclet number which is defined as:

$$\xi = \pm\frac{T_c}{1+M^2}\frac{Ra}{Pe} \tag{11}$$

where, $M^2 = \frac{k\sigma {B_0}^2}{\mu}$ is the Hartmann number, $Ra = \frac{gk\gamma\rho_c}{\mu\alpha_m}T_c$ is the modified Rayleigh number and $Pe = \frac{\mu_\infty}{\alpha_m}$ being the Peclet number. The primes denote differentiation with respect to the similarity variable η: The wall temperature condition 5(a)–5(c) leads to $\theta(0) = 1$, or $\theta'(0) = -Pe^{1/2}$ or $\theta(0) + Pe^{1/2}\theta'(0) = 0$. The velocity filed $v = (u, v, 0)$ is expressed in terms of f and f':

$$u(x,y) = u_e(x)f'(\eta), v(x,y) = -\frac{\alpha_m}{2x}Pe_x^{1/2}[(2m-1)\eta f'(\eta) + (2m+1)f(\eta)] \tag{12}$$

Note that the parameter ξ determines the physical phenomenon is one of the forced convection $\xi = 0$ free convection $\xi \to \infty$ or mixed convection $\xi \neq 0$.

Optimal Homotopy Analysis Method (OHAM)

In order to obtain the convergence of current model, we have imposed HAM that is dealing the values of convergence control parameters. To optimize the involved emerging parameters, OHAM is applied in the given domain. For this determination, we have obtained discrete squared residual error for kth iteration that is presented by Ref. [31], Tables 1 and 2

Table 1 – Total average square residual errors for $m = 0.2$, $\xi = 0.3$.

k = Number of iteration	$\hbar_f$	$\hbar_\theta$	E_k^t	CPU time (sec)
04	−1.3847	−1.3663	2.0516×10^{-4}	15.110
06	−1.5657	−1.4782	5.5545×10^{-5}	72.150
10	−1.6921	−1.6162	4.7439×10^{-6}	869.45

Table 2 – Individual averaged square residual errors using optimal values at k=10.

k = Number of iteration	E_k^f	E_k^θ	CPU time (sec)
04	4.4539×10^{-7}	6.6705×10^{-5}	09.38
06	1.8719×10^{-9}	6.8904×10^{-6}	44.98
10	5.8288×10^{-8}	4.7389×10^{-6}	48.15

Please cite this article in press as: Ul Haq R, et al., MHD mixed convection flow along a vertically heated sheet, International Journal of Hydrogen Energy (2017), http://dx.doi.org/10.1016/j.ijhydene.2017.04.225

$$E_k^f \approx \frac{1}{N+1}\sum_{j=0}^{N}\left\{N_f\left[\sum_{i=0}^{k} f_i(\eta_j), \sum_{i=0}^{k}\theta_i(\eta_j)\right]\right\}^2, \tag{13}$$

$$E_k^\theta \approx \frac{1}{N+1}\sum_{j=0}^{N}\left\{N_f\left[\sum_{i=0}^{k} \theta_i(\eta_j), \sum_{i=0}^{k} f_i(\eta_j)\right]\right\}^2, \tag{14}$$

where $\eta_j = j\Delta\eta$, $\Delta\eta = 0.5$ and $N = 20$. The total discrete square residual error, defined as:

$$E_k^{total} = E_k^f + E_k^\theta, \tag{15}$$

$$\frac{\partial E_k^{total}}{\partial \hbar_f} = \frac{\partial E_k^{total}}{\partial \hbar_\theta} = 0, \tag{16}$$

Numerical technique

Numerical approach has been proposed to validate the obtained optimized solutions through two different analytical techniques HAM and OHAM. System of coupled differential Eqs. (9a) and (9b) with the boundary condition (10) are converted into the initial value problem by shooting method and then solve that system with the help of Runge–Kutta–Fehlberg method. The procedure of shooting method is mentioned below:

To convert the boundary value problem to initial value problem we need to fix

$$f'(\eta) = p,\ f''(\eta) = p' = q,\ \theta'(\eta) = r,\ \theta''(\eta) = r' = s.$$
$$p = 1 + \xi\theta(\eta)^2, \tag{17}$$

$$s = mf'(\eta)\theta(\eta) - \frac{1+2m}{2} rf(\eta). \tag{18}$$

The associated initial conditions are as follows:

$$f(0) = 0,\ \ \theta(0) = 0. \tag{19}$$

To determine the missing condition at $\eta \to \infty$, we integrate Eqs. (17) and (18) with the initial condition (19), the values of $p(0) = f'(0) = \alpha$ and $r(0) = \theta'(0) = \beta$ are required. The suitable guess for $p(0)$ and $r(0)$ are chosen and then integration is performed. For this particular model step size is considered as $\Delta\eta = 0.01$ and the convergence criteria were set to 10^{-6}.

Method's compatibility

Before going to discuss the result analysis, it better to validate both numerical and OHAM result. For this, results are plotted in Fig. 2, both velocity and temperature profile for (a) $m = 0.2$, $\xi = 0.3$ and (b) $m = -0.25$, $\xi = 0.4$. One can see that results produced by numerical approach are in good agreement with Optimal Homotopy Analysis Method (OHAM) (see Fig. 2).

Comparison of results

In order to validate our present study with the existing literature, we have made a comparison with the results published by Guedda et al. [30]. One can see that present obtained results via OHAM are showing the excellent agreement for each velocity and temperature profile (see Fig. 3). It can further observed that present study demonstrate the better convergence, more stable and long lasting results as compare to results obtained by Guedda et al. [30]. Furthermore, present established results are accurately satisfying the boundary conditions for both momentum and energy equations.

Results and discussion

In order to investigate the fluid behavior within the boundary layer thickness, results are plotted for $f(\eta)$ for various values of emerging parameters ξ and m (see Fig. 4). Here in Fig. 4, results

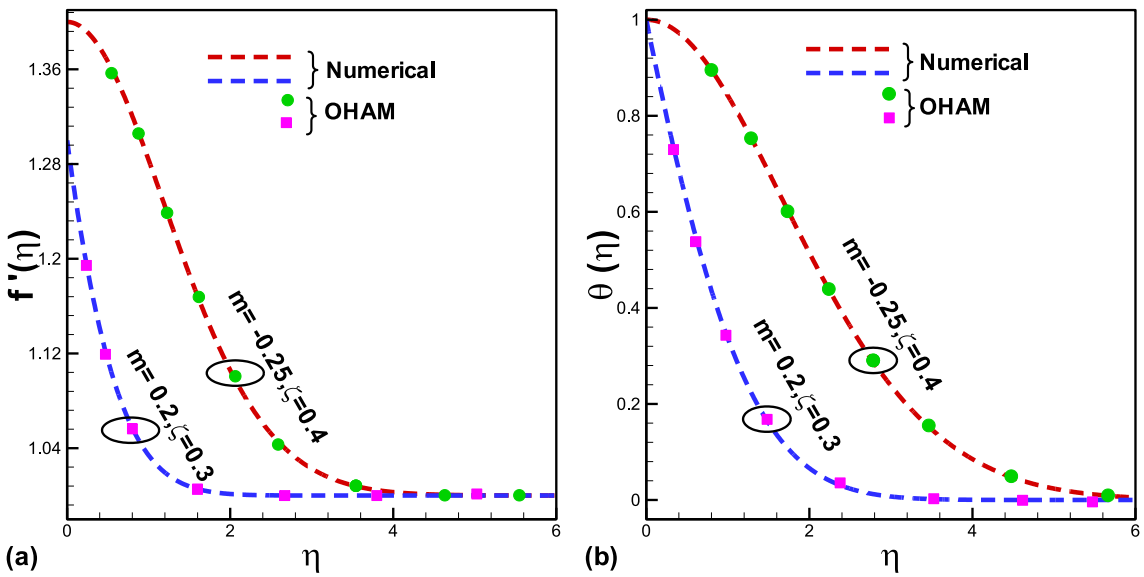

Fig. 2 – Comparison between numerical and OHAM approach for (a) velocity profile and (b) temperature profile.

Please cite this article in press as: Ul Haq R, et al., MHD mixed convection flow along a vertically heated sheet, International Journal of Hydrogen Energy (2017), http://dx.doi.org/10.1016/j.ijhydene.2017.04.225

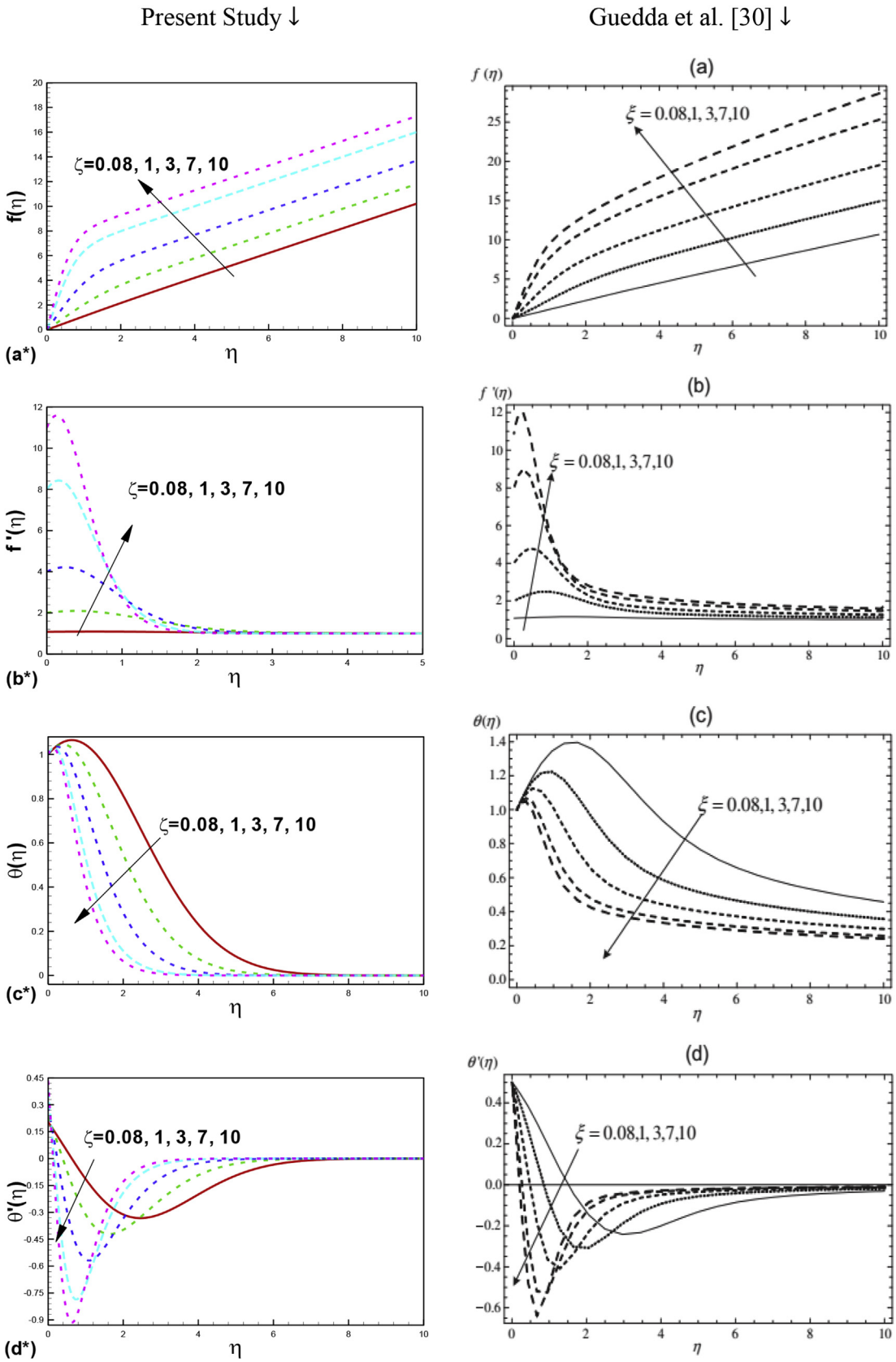

Fig. 3 – Comparison of (a*)–(d*) Present study with (a)–(d) Guedda et al. [30] for $m = -0.2$.

Please cite this article in press as: Ul Haq R, et al., MHD mixed convection flow along a vertically heated sheet, International Journal of Hydrogen Energy (2017), http://dx.doi.org/10.1016/j.ijhydene.2017.04.225

are classifying according for $\xi<0$, $\xi>0$ and $\xi=0$ for $m=-0.2$, 0 and 0.2. Through results it can easily determine that effects of m are not significant for $f(\eta)$. But in the inset it can be figure out that there is a slight increase in the $f(\eta)$ when $(\xi<0)$. However variation in the results of $f(\eta)$ are opposite for increasing values of m when $(\xi>0)$. Since there are three physical parameters namely: MHD parameter M, modified Rayleigh number *Ra* and the Peclet number *Pe* are merged in a single parameter ξ. So the combine effect of all this parameters can be visualized with the variation of ξ. Again it can be observed through Fig. 4 that there is an increase in the $f(\eta)$ with simultaneous increase in ξ with m.

Variation of the velocity profile $f(\eta)$ for various values of ξ and m are plotted in Fig. 5. It is observed that the behavior of velocity profile $f'(\eta)$ remains same in Fig. 5 for each value of m, when these are compared with Fig. 4. Results obtained in Fig. 5 depict the effects of m which are very dominant on velocity variation. It is found that for $(\xi>0)$, graphs for velocity profile shows the decreasing behavior for increasing value of m. On the other side when $(\xi<0)$, results produced for velocity are showing the increasing behavior for each increasing values of m. Fig. 5 also depicts that the behavior of boundary layer thickness is getting reduce for each value of physical parameter. However, when $\xi=0$ then the behavior of the velocity profile remains uniform that is $(f(\eta)=1)$. Simultaneous effects of emerging parameters ξ and m on temperature profile $\theta(\eta)$ are plotted in Fig. 6. Falling of temperature described that there is loss of energy due to increase in the power index m. Physically, higher values of power index m show the increase in the free stream velocity. Consequently, heat will disperse because of higher disturbance in the fluid. It is further determine that behavior of $\theta(\eta)$ for each value of ξ is getting decrease. Since ξ is ratio of Rayleigh to Peclet number so increase in ξ implies increase of Rayleigh number that decrease the temperature profile within the boundary layer. Moreover we can further observe that for each value of ξ and m, thermal boundary layer decreases gradually.

The 3-Dimension behavior of streamlines pattern is plotted for $u(x, y)$ and $v(x, y)$ in Fig. 7(a) and (b), respectively. Here results are generated for various value of m while value of ξ is kept fixed. As from Fig. 7(a), it can be observed that stream line which is constructed for $m=-0.25$ is intersecting the rest of stream lines at $x=1$. Further, it is found that with the simultaneous increase in $x-$ and $y-$ directions gives the dominant variation in the stream lines along $v(x, y)$. It can be analyzed that results produced in Fig. 7 shows the dispersion of $v(x, y)$ for each value of $m=-0.25$, 0, 0.10 and 0.25 at $v=0$. To analyze the fluid flow parameter, results are plotted in the form of stream lines (see Figs. 8 and 9). These results are plotted within the boundary layer region for various values of emerging parameters m and ξ. Further it is determined that

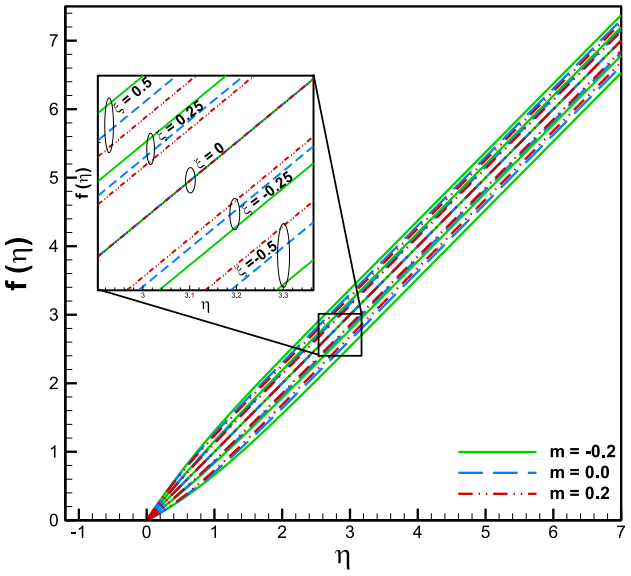

Fig. 4 – Variation of $f(\eta)$ for various values of ξ and m.

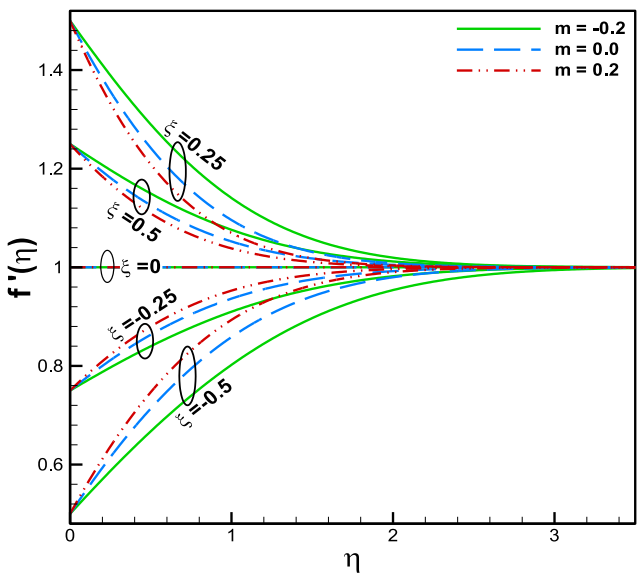

Fig. 5 – Variation of $f'(\eta)$ for various values of ξ and m.

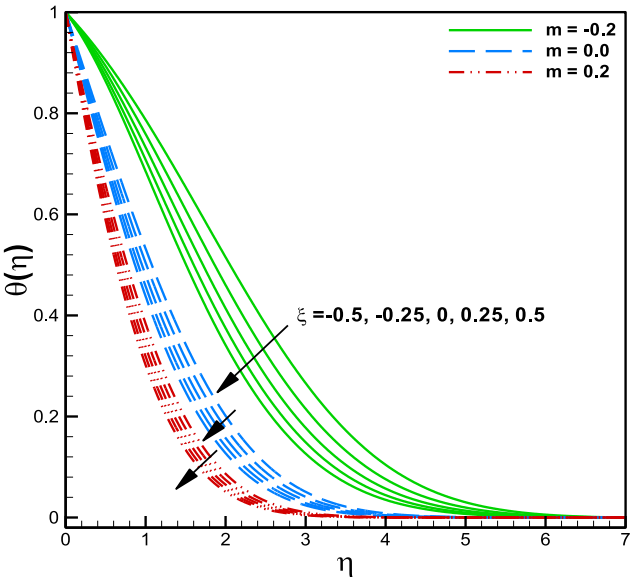

Fig. 6 – Variation of $\theta(\eta)$ for various values of ξ and m.

Please cite this article in press as: Ul Haq R, et al., MHD mixed convection flow along a vertically heated sheet, International Journal of Hydrogen Energy (2017), http://dx.doi.org/10.1016/j.ijhydene.2017.04.225

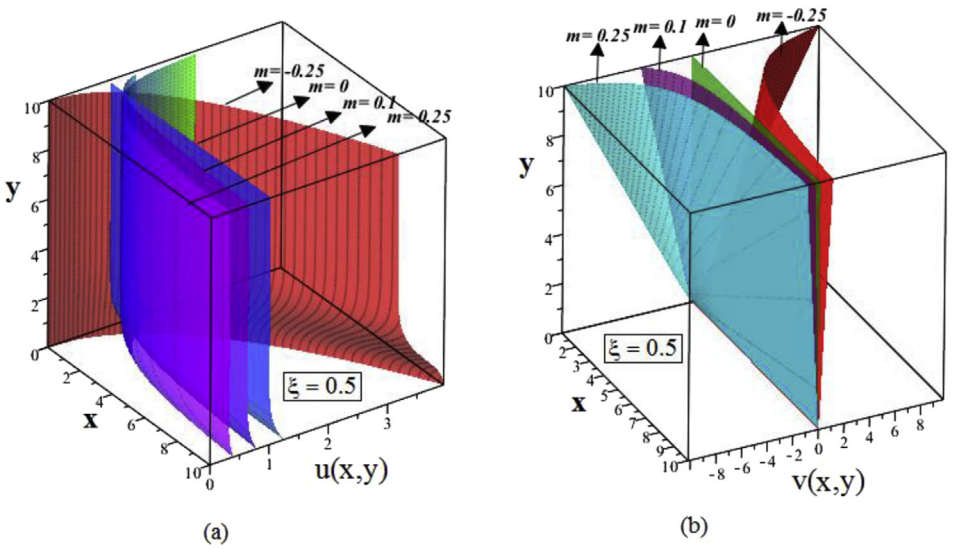

Fig. 7 – 3-D view of stream lines for various values of m (a) $u(x, y)$ and (b) $v(x, y)$.

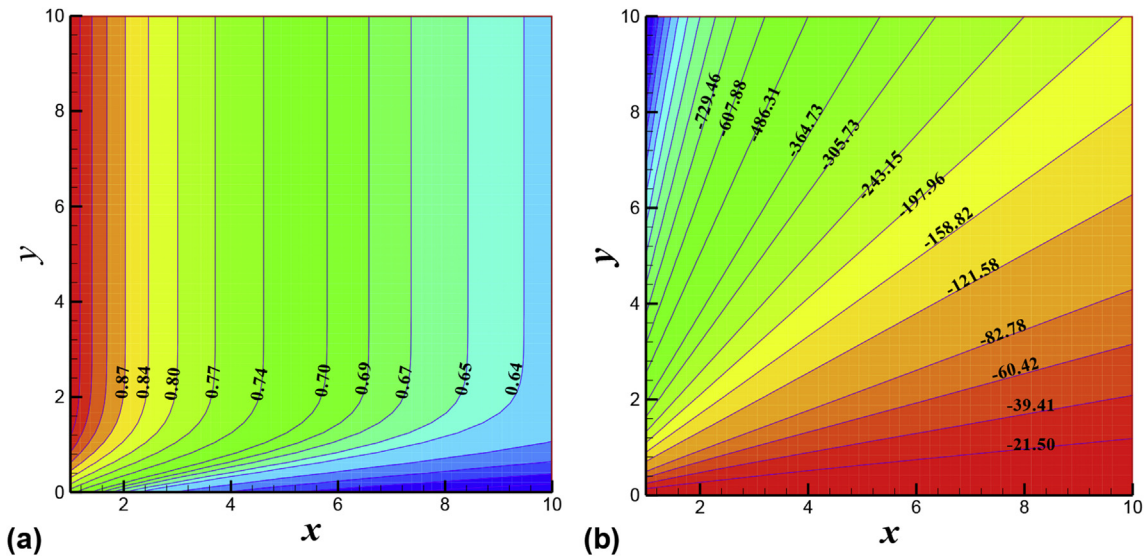

Fig. 8 – Variation of (a) $u(x, y)$ and (b) $v(x, y)$ when (m=0.1, $\xi = -0.25$).

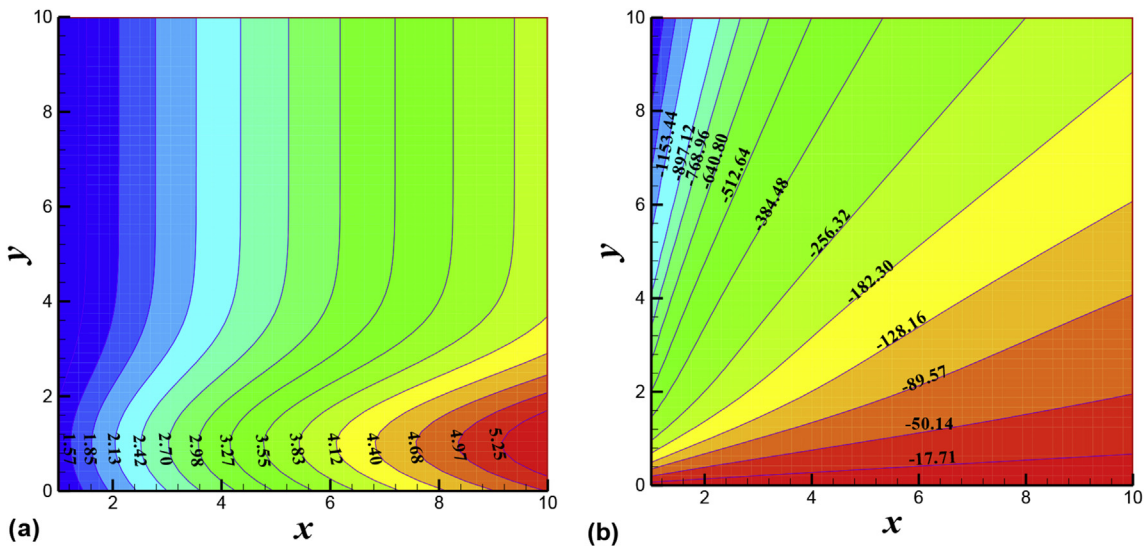

Fig. 9 – Variation of (a) $u(x, y)$ and (b) $v(x, y)$ when (m=−0.3, $\xi = 0.25$).

Please cite this article in press as: Ul Haq R, et al., MHD mixed convection flow along a vertically heated sheet, International Journal of Hydrogen Energy (2017), http://dx.doi.org/10.1016/j.ijhydene.2017.04.225

the variation of velocity profiles along x and y directions gives the very dominant effects in stream pattern that based on negative and positive values of emerging parameters.

Conclusion

In this article we have deal the MHD mixed convection flow along a heated wall that is filled with the porous media at 4 °C. Significant effects of wall temperature are determined for temperature profile in the restricted semi-infinite domain. Governing partial differential equations are rehabilitated in the form of ordinary differential equation via suitable transformation. Results are obtained via two separate techniques: numerically with the help of shooting technique and verified with the help of OHAM. Mixed convection parameter ξ plays a most dominating role on the whole analysis. It can be found that for $\xi < 0$, velocity profile depicts the increasing behavior for various values of m. However, for $\xi > 0$, velocity profile shows the decreasing behavior with respect the parameter m. Temperature distribution in the restricted domain depicts the decreasing behavior for m and ξ. Results obtained from both numerical and analytical techniques depict the excellent agreement.

REFERENCES

[1] Sparrow EM, Eichhorn R, Gregg JL. Combined forced and free convection in boundary layer flow. Phys Fluids 1959;2:319–28.
[2] Merkin JH, Pop I. Mixed convection along a vertical surface: similarity solutions for uniform flow. Fluid Dyn Res 2002;30:233–50.
[3] Nadeem S, Saleem S. Mixed convection flow of Eyring–Powell fluid along a rotating cone. Results Phys 2014;4:54–62.
[4] Noor NFM, Ul Haq Rizwan, Nadeem S, Hashim I. Mixed convection stagnation flow of a micropolar nanofluid along a vertically stretching surface with slip effects. Meccanica 2015;50(8):2007–22.
[5] Aly EH, Elliott L, Ingham DB. Mixed convection boundary-layer flow over a vertical surface embedded in a porous medium. Eur J Mech B Fluids 2003;22:529–43.
[6] Vargas JVC, Laursen TA, Bejan A. Nonsimilar solutions for mixed convection on a wedge embedded in a porous medium. Int J Heat Fluid Flow 1995;16:211–6.
[7] Nield DA, Bejan A. Convection in porous media. 2nd ed. New York: Springer; 1999.
[8] Ingham DB, Pop I, editors. Transport phenomena in porous media. Oxford: Pergamon; 1998. vol. II (2002), vol. III (2005).
[9] Vafai K, editor. Handbook of porous media. New York: Marcel Dekker; 2000.
[10] Kumaran V, Pop I. Steady free convection boundary layer over a vertical flat plate embedded in a porous medium filled with water at 4°C. Int J Heat Mass Transf 2006;49:3240–52.
[11] Lide David R. Handbook of chemistry and physics. 65th ed. Boca Raton, Florida: CRC Press; 1984.
[12] Goren L. On free convection in water at 4° C. Chem Eng Sci 1966;21:515–8.
[13] Moore DR, Weiss NO. Non-linear penetrative convection. J Fluid Mech 1973;61:553–81.
[14] Gebhart B, Mollendorf JC. A new density relation for pure and saline water. Deep Sea Res 1977;24:831–48.
[15] Georgantopoulos G, Nanousis N, Douskos C. Hy-dromagnetic free convection effects on the oscillatory flow of water at 4°C past an infinite porous plate. Rev Roumaine Phys 1982;26:39–58.
[16] Takhar HS, Perdikis CP. Forced and free convection flow of water at 4°C through a porous medium. Int Commun Heat Mass Transf 1986;13:605–9.
[17] Xenos Michalis, Dimas Stelios, Raptis Andreas. MHD free convective flow of water near 4°C past a vertical moving plate with constant suction. Appl Math 2013;4:52–7.
[18] Ellahi R, Shivanian E, Abbasbandy S, Hayat T. Analysis of some magnetohydrodynamic flows of third order fluid saturating porous space. J Porous Media 2015;18(2):89–98.
[19] Rashidi S, Nouri-Borujerdi A, Valipour MS, Ellahi R, Pop I. Stress jump and continuity interface conditions for a cylinder embedded in a porous medium. Transp Porous Media 2015;107(1):171–86.
[20] Shirvan KM, Ellahi R, Mirzakhanlari S, Mamourian M. Enhancement of heat transfer and heat exchanger effectiveness in a double pipe heat exchanger filled with porous media: numerical simulation and sensitivity analysis of turbulent fluid flow. Appl Therm Eng 2016;109:761–74.
[21] Ellahi R. The effects of MHD and temperature dependent viscosity on the flow of non-Newtonian nanofluid in a pipe: analytical solutions. Appl Math Model 2013;37(3):1451–7.
[22] Ellahi R, Bhatti MM, Pop I. Effects of hall and ion slip on MHD peristaltic flow of jeffrey fluid in a non-uniform rectangular duct. Int J Numer Methods Heat Fluid Flow 2016;26(6).
[23] Ellahi R, Shivanian E, Abbasbandy S, Hayat T. Numerical study of magnetohydrodynamics generalized Couette flow of Eyring-Powell fluid with heat transfer and slip condition. Int J Numer Methods Heat Fluid Flow 2016;26(5):1433–45.
[24] Rashidi S, Dehghan M, Ellahi R, Riaz M, Jamal-Abad MT. Study of stream wise transverse magnetic fluid flow with heat transfer around a porous obstacle. J Magn Magn Mater 2015;378:128–37.
[25] Sheikholeslami M, Ganji DD. Influence of magnetic field on CuO–H_2O nanofluid flow considering Marangoni boundary layer. Int J Hydrogen Energy 2017;42(5):2748–55.
[26] Chernova NI, Kiseleva SV. Microalgae biofuels: induction of lipid synthesis for biodiesel production and biomass residues into hydrogen conversion. Int J Hydrogen Energy 2017;42(5):2861–7.
[27] Rasheed Raj Kamal Abdul, Liao Quan, Caizhi Zhang, Chan Siew Hwa. A review on modelling of high temperature proton exchange membrane fuel cells (HT-PEMFCs). Int J Hydrogen Energy 2017;42(5):3142–65.
[28] Hou Y, Zhang G, Qin Y, Du Q, Jiao K. Numerical simulation of gas liquid two-phase flow in anode channel of low-temperature fuel cells. Int J Hydrogen Energy 2017;42(5):3250–8.
[29] Burheim OS, Su H, Hauge HH, Pasupathi S, Pollet BG. Study of thermal conductivity of PEM fuel cell catalyst layers. Int J Hydrogen Energy 2014;39(17):9397–408.
[30] Guedda M, Aly Emad H, Ouahsine A. Analytical and ChPDM analysis of MHD mixed convection over a vertical flat plate embedded in a porous medium filled with water at 4°C. Appl Math Model 2011;35:5182–97.
[31] Liao SJ. An optimal homotopy analysis approach for strongly nonlinear differential equations. Commun Nonlinear Sci Numer Simul 2010;15:2016.

Please cite this article in press as: Ul Haq R, et al., MHD mixed convection flow along a vertically heated sheet, International Journal of Hydrogen Energy (2017), http://dx.doi.org/10.1016/j.ijhydene.2017.04.225